

# All-fiber tunable filter and laser based on two-mode fiber

Seok Hyun Yun, In Kag Hwang, and Byoung Yoon Kim

*Department of Physics, Korea Advanced Institute of Science and Technology,  
373-1, Kusong-dong, Yuseong-gu, Taejeon 305-701, Korea*

Received October 18, 1995

We demonstrate an all-fiber acousto-optic tunable filter based on two-spatial-mode coupling, with improved ruggedness and efficiency, by using a new acoustic-transducer design. We use a rigorous modeling of the flexural acoustic wave to analyze the mode coupling with better accuracy. Using the acousto-optic tunable filter, we demonstrate a novel all-fiber tunable laser with a tuning range of more than 20 nm and a linewidth of 0.2 nm. © 1996 Optical Society of America

Acousto-optic devices have been investigated with growing interest for their use as tunable-wavelength filters or switches in fiber-optic wavelength-division-multiplexed systems. One attractive approach is based on the interaction of a surface acoustic wave and two optical polarization modes guided in an integrated LiNbO<sub>3</sub> waveguide. Quite complex waveguide designs are needed for good sidelobe suppression and low polarization dependence.<sup>1</sup> Such devices also demonstrate a large insertion loss of a few decibels, mainly because of the coupling loss at the junctions between the waveguide and the optical fibers.

The same operating principle can be realized in an all-fiber form based on coupling between two spatial optical modes, instead of two polarization modes, by a flexural acoustic wave.<sup>2-5</sup> The all-fiber configuration leads to a very low insertion loss because a simple fusion splicing can be used to connect the device to other fiber-optic systems. The use of two spatial modes makes it much simpler to design a polarization-insensitive device. In this Letter, we demonstrate and characterize an all-fiber acousto-optic tunable filter (AOTF) with improved mechanical ruggedness and efficiency based on a new acoustic-transducer design. We describe our finding that corrections are needed to published theoretical predictions of the coupling efficiency.<sup>6</sup> We also demonstrate the application of the AOTF to a novel wavelength-tunable all-fiber laser.

As has been shown elsewhere,<sup>2</sup> the lowest-order flexural acoustic wave propagating along a two-mode fiber produces periodic microbends, causing mode coupling between the fundamental and the second-order modes. The details of the acoustic-wave propagation in a fiber are well described in Ref. 3. In the following analysis we used coupled-mode theory<sup>7</sup> to calculate the efficiency of mode coupling provided by the flexural acoustic wave. The two coupled optical modes were approximated as the LP<sub>01</sub> and the LP<sub>11</sub> modes, which is valid for a weakly guiding fiber. For simplicity the lobe orientation of the LP<sub>11</sub> mode was assumed to be aligned with the direction of acoustic displacement. When only the LP<sub>01</sub> mode is launched into the fiber in the presence of the acoustic wave, the conversion efficiency  $P(L)$ , defined as the ratio of the coupled LP<sub>11</sub> mode intensity to the total intensity

after coupling length  $L$ , becomes<sup>7</sup>

$$P(L) = \frac{\gamma^2}{\gamma^2 + (\theta/2)^2} \sin^2\{[\gamma^2 + (\theta/2)^2]^{1/2}L\}. \quad (1)$$

Here  $\theta = 2\pi(1/\lambda_a - 1/L_B)$  represents the magnitude of the phase mismatch, where  $\lambda_a$  is the acoustic wavelength and  $L_B$  is the beat length between the two modes.

We calculate the coupling coefficient  $\gamma$  by taking into account the antisymmetric optical path variations caused by the geometrical microbends and the strain-induced refractive-index change. For a circular-core step-index fiber  $\gamma$  can be expressed as

$$\gamma = \frac{\delta_a(1 - \chi)}{a} Y(V) \frac{L_B}{\lambda_a^2}. \quad (2)$$

Here  $\delta_a$  is the transverse-displacement amplitude of the acoustic wave at the core,  $a$  is the core radius, and  $V = (2\pi/\lambda)a(n_{co}^2 - n_{cl}^2)^{1/2}$  is the normalized frequency, where  $\lambda$  is the optical wavelength and  $n_{co}$  and  $n_{cl}$  are the refractive indices of the core and the cladding, respectively. The parameter  $\chi$  accounts for the refractive-index change caused by the acoustic strain through the elasto-optic effect, which tends to reduce the mode coupling induced by the geometrical effect. The values of  $\chi$  are calculated by the acoustic-wave equation<sup>3</sup> and are plotted in Fig. 1(a) for two orthogonal optical polarizations as a function of  $D/\lambda_a$ , where  $D$  is the fiber diameter. When  $D \ll \lambda_a$ ,  $\chi \approx 0.22$  for a silica glass fiber, as is described in Ref. 6. However, we point out that  $\chi$  is a function of  $D/\lambda_a$  and decreases as  $D/\lambda_a$  increases. We can understand this by considering that the acoustic-strain effect comes mainly from the axial displacement of the acoustic wave, and it approaches zero at the fiber core as  $D/\lambda_a$  increases. The function  $Y(V)$ , which depends only on the normalized frequency  $V$ , is plotted in Fig. 1(b). The value of  $\gamma$  is larger by a factor of 1.1–1.5 than the previous result<sup>6</sup> in the practical range,  $0 < D/\lambda_a < 1$ . The discrepancy is attributed to the circular-microbend modeling of the acoustic wave instead of the exact sinusoidal displacement used here and to errors in calculating the bend angle and the coupling coefficient in Ref. 6.

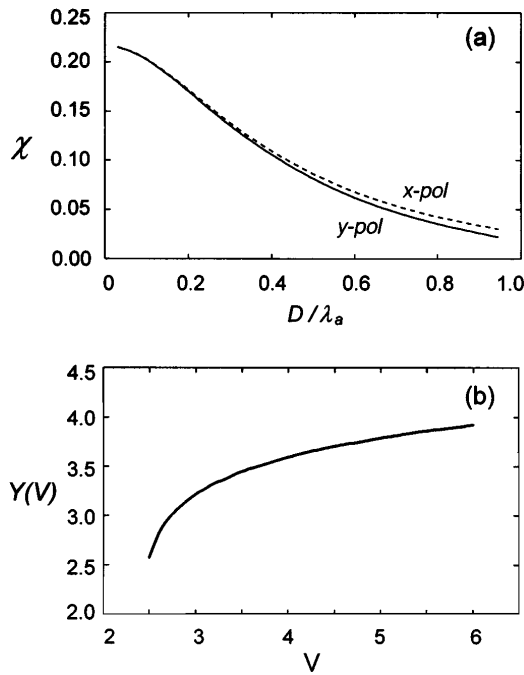


Fig. 1. (a) Calculated values of  $\chi$  for silica glass fiber as a function of the ratio of the fiber diameter to the acoustic wavelength,  $D/\lambda_a$ . The transverse acoustic displacement is assumed to be in the  $y$  direction. (b) The function  $Y(V)$  calculated for a circular-core step-index fiber.

For a given acoustic wavelength the mode-conversion efficiency depends on the optical wavelength through the  $\lambda$  dependence of the beat length. Therefore, by ensuring that one mode enters the coupling region and by selecting or eliminating the other mode after the coupling region, we can choose or reject an optical signal only within a narrow spectral range. We can tune the center wavelength of the bandpass or notch filter by controlling the acoustic frequency. The 3-dB bandwidth of the filter derived from Eq. (1) is<sup>5</sup>

$$\left(\frac{\Delta\lambda}{\lambda}\right)_{3\text{dB}} \approx \frac{0.8}{m} \frac{L_B}{\lambda} \frac{d\lambda}{dL_B}, \quad (3)$$

where  $m = L/L_B$  is defined as the number of beats in the coupling region of length  $L$ .

Figure 2 shows a schematic diagram of an experimental AOTF in a notch-filter configuration. The flexural acoustic wave generated by an acoustic transducer is guided along an unjacketed section of a fiber and is then absorbed by an acoustic damper. The newly designed coaxial acoustic transducer consisted of a glass horn, a piezoelectric transducer (PZT), and a heat sink. We prepared the cone-shaped acoustic horn by tapering a 1-cm-long capillary with a 4.5-mm outer diameter and a 150- $\mu\text{m}$  inner diameter. A shear-mode PZT slab was bonded to the horn base, and an aluminum plate attached to the PZT acted as a heat sink as well as a mount. The shear-mode PZT is more effective than the previously demonstrated thickness-mode PZT<sup>8</sup> for exciting the flexural acoustic wave in the horn because of a better acoustic mode match. All three components had holes in their centers such that an unjacketed fiber could be inserted and bonded to them. We prepared the fiber by draw-

ing a preform that was designed for a conventional single-mode communication fiber to a diameter of 136  $\mu\text{m}$  with a single-mode cutoff wavelength of  $\sim 1.4 \mu\text{m}$ . The length of the unjacketed fiber was 11.5 cm, which defined the acousto-optic interaction region. The first mode stripper formed by tight bends of the fiber permits only the  $\text{LP}_{01}$  mode to enter the coupling region. The second mode stripper is used to eliminate the  $\text{LP}_{11}$  mode generated by the mode coupling.

The center wavelength of the notch filter as a function of the acoustic frequency is plotted in Fig. 3. Complete mode coupling was obtained at the optical wavelengths 0.9–1.1  $\mu\text{m}$ . At other wavelengths the mode coupling was limited mainly by the finite bandwidth of the PZT resonance. The required electrical drive power for complete mode coupling was 25–75 mW over the 200-nm spectral range 0.9–1.1  $\mu\text{m}$ . The device did not have strong acoustic resonances because of good acoustic impedance matching between the fiber and the horn. The efficiency can be improved further for a much-limited acoustic-frequency range if a strong acoustic resonance is generated and used.<sup>4</sup> The transverse acoustic amplitude  $\delta_a$  required for the complete mode conversion is estimated from Eq. (2) to be  $\sim 13 \text{ nm}$ , which corresponds to an acoustic power of  $\sim 4 \text{ mW}$ .<sup>3</sup>

Figure 4 shows the spectral response of the notch filter obtained by use of fluorescent light from a  $\text{Nd}^{3+}$ -doped fiber as a broadband optical source and measurement of transmitted power with an optical spectrum analyzer. At an acoustic frequency of 3.100 MHz, where  $\lambda_a \approx 570 \mu\text{m}$ , mode coupling occurred at  $\lambda = 1060 \text{ nm}$  with a 3-dB optical band-

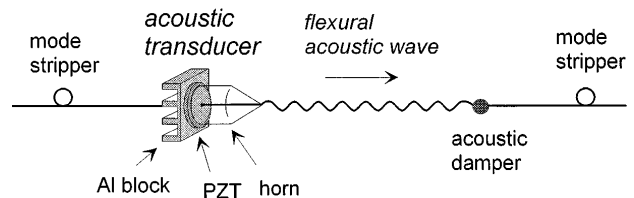


Fig. 2. Schematic diagram of the all-fiber AOTF with a new acoustic transducer.

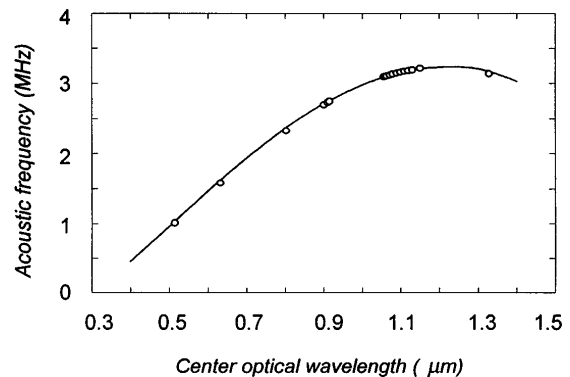


Fig. 3. Measured center wavelength of the notch filter as a function of the acoustic frequency. The theoretical curve shows good agreement with the experimental data (circles); a circular-core step-index profile with a central dip is assumed.

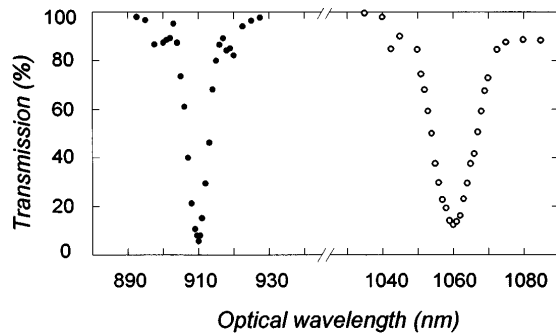


Fig. 4. Spectral response of the AOTF measured with an unpolarized broadband light at  $f_a = 2.726$  MHz (●) and  $f_a = 3.100$  MHz (○).

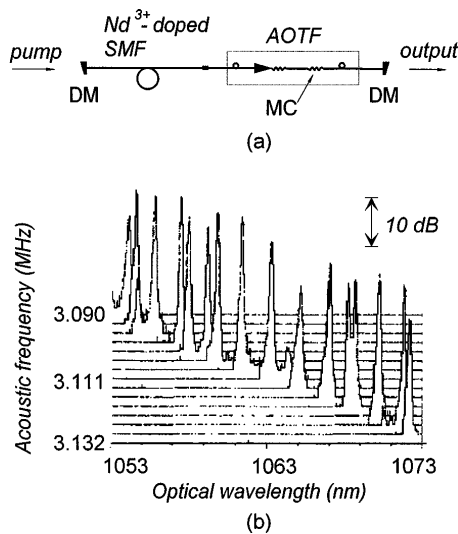


Fig. 5. (a) Schematic diagram of the all-fiber tunable laser: DM's, dichroic mirrors; MC, static mode converter; SMF, single-mode fiber. (b) Spectrum of the laser output tuned by variation of the acoustic frequency.

width of 13.7 nm. At an acoustic frequency of 2.726 MHz, where  $\lambda_a \approx 620 \mu\text{m}$ , mode coupling occurred at  $\lambda = 910$  nm with a bandwidth of 6.7 nm. The nonzero transmission at the peak coupling was due to the small polarization dependence of the device.<sup>5</sup> The insertion loss of the device caused by mode coupling to cladding modes at various acoustic frequencies at  $\lambda = 1064$  nm was  $\sim 0.35$  dB in the worst case.

As an application of the AOTF, we constructed a novel all-fiber tunable laser by using a bandpass configuration having a static mode converter before the second mode stripper,<sup>4-6</sup> as shown in Fig. 5(a). We constructed the static mode converter by squeezing the fiber with two corrugated plates, which had  $\sim 30$  grooves of 570- $\mu\text{m}$  period. The gain was provided by a 4-m-long  $\text{Nd}^{3+}$ -doped single-mode fiber pumped at  $\lambda = 807$  nm. The total cavity loss was measured to be  $\sim 3$  dB per single pass, which came mainly from the mode strippers and a splice between

two dissimilar fibers. Light inside the laser cavity experiences a frequency shift of twice the acoustic frequency per round trip. The frequency-shifted feedback can produce continuous-wave output without the usual longitudinal cavity modes.<sup>9</sup> However, mode-locked pulses can also be produced either by the Kerr-type fiber nonlinearity at a strong pump-power level<sup>10</sup> or by the residual unshifted-frequency components caused by the imperfection of the AOTF. The latter is significant if the acoustic frequency or its harmonics match the longitudinal mode spacing. In our experiment a continuous-wave output was obtained at acoustic frequencies of  $\sim 3.11$  MHz, when the longitudinal mode spacing was 8.4 MHz and the pump power was less than 1.3 times the threshold pump power of 18 mW. As the acoustic frequency was varied, the optical wavelength was tuned with a slope coefficient of  $\sim 0.5$  nm/kHz in the tuning range of more than 20 nm, as shown in Fig. 5(b). The average output power was 0.15 mW at the pump-power level of 23 mW. The linewidth of the laser was less than 0.2 nm over the whole tuning range, much narrower than that of the AOTF itself, even though double spectral peaks appeared at some acoustic frequencies. The laser output was stable in the laboratory environment, but the change in the fiber birefringence caused a lasing wavelength shift by as much as a few nanometers that could be suppressed by elimination of the polarization dependence of the AOTF.

In conclusion, using a new coaxial acoustic transducer, we have demonstrated an all-fiber AOTF that has improved efficiency and ruggedness. The coupling efficiency was calculated theoretically by coupled-mode analysis, leading to a correction factor of  $\sim 1.3$  compared with the published results.<sup>6</sup> We demonstrated a novel tunable all-fiber laser using the AOTF as a tuning element.

## References

1. H. Herrmann, K. Schafer, and W. Sohler, *IEEE Photon. Technol. Lett.* **11**, 1135 (1994).
2. B. Y. Kim, J. N. Blake, H. E. Engan, and H. J. Shaw, *Opt. Lett.* **11**, 389 (1986).
3. H. E. Engan, B. Y. Kim, J. N. Blake, and H. J. Shaw, *J. Lightwave Technol.* **6**, 428 (1988).
4. J. N. Blake and P. Siemsen, presented at Ninth Optical Fiber Sensors Conference, Firenze, Italy, 1993.
5. D. Ostling and H. E. Engan, *Opt. Lett.* **20**, 1247 (1995).
6. J. N. Blake, B. Y. Kim, H. E. Engan, and H. J. Shaw, *Opt. Lett.* **12**, 281 (1987).
7. A. Yariv and P. Yeh, *Optical Waves in Crystals* (Wiley, New York, 1987), Chap. 6.
8. O. Lisboa, J. N. Blake, J. E. B. Oliveira, and S. L. A. Cararra, *Proc. Soc. Photo-Opt. Instrum. Eng.* **1267**, 17 (1990).
9. P. F. Wysocki, M. J. K. Dignonet, and B. Y. Kim, *Opt. Lett.* **15**, 273 (1990).
10. H. Sabert and E. Brinkmeyer, *J. Lightwave Technol.* **12**, 1360 (1994).